CpG-induced tyrosine phosphorylation occurs via a TLR9-independent mechanism and is required for cytokine secretion

Miguel A. Sanjuan,[1] Navin Rao,[1] Kuei-Tai A. Lai,[1] Yin Gu,[1] Siquan Sun,[1] Anja Fuchs,[2] Wai-Ping Fung-Leung,[1] Marco Colonna,[2] and Lars Karlsson[1]

[1]Johnson & Johnson Pharmaceutical Research and Development, L.L.C., San Diego, CA 92121
[2]Department of Pathology and Immunology, Washington University School of Medicine, St. Louis, MO 63110

Toll-like receptors (TLRs) recognize molecular patterns preferentially expressed by pathogens. In endosomes, TLR9 is activated by unmethylated bacterial DNA, resulting in proinflammatory cytokine secretion via the adaptor protein MyD88. We demonstrate that CpG oligonucleotides activate a TLR9-independent pathway initiated by two Src family kinases, Hck and Lyn, which trigger a tyrosine phosphorylation–mediated signaling cascade. This cascade induces actin cytoskeleton reorganization, resulting in cell spreading, adhesion, and motility. CpG-induced actin polymerization originates at the plasma membrane, rather than in endosomes. Chloroquine, an inhibitor of CpG-triggered cytokine secretion, blocked TLR9/MyD88-dependent cytokine secretion as expected but failed to inhibit CpG-induced Src family kinase activation and its dependent cellular responses. Knock down of Src family kinase expression or the use of specific kinase inhibitors blocked MyD88-dependent signaling and cytokine secretion, providing evidence that tyrosine phosphorylation is both CpG induced and an upstream requirement for the engagement of TLR9. The Src family pathway intersects the TLR9–MyD88 pathway by promoting the tyrosine phosphorylation of TLR9 and the recruitment of Syk to this receptor.

Introduction

Upon recognizing pathogen-associated molecular patterns, the family of 11 Toll-like receptors (TLRs) provides the initial activation signal to the immune system, resulting in costimulatory molecule expression and cytokine secretion (Krieg, 2002a; Takeda et al., 2003). These cytokines can modulate the adaptive immune response to eliminate particular classes of pathogens by polarizing CD4$^+$ T cells to either a Th1 or -2 phenotype (Krieg, 2002b). However, an unbalanced or sustained Th1 or -2 response can lead to diseases such as rheumatoid arthritis and asthma (Trinchieri, 2003).

The pathogen-associated molecular pattern of unmethylated bacterial DNA is specifically recognized by TLR9, and its immunomodulatory effects can be mimicked by oligodeoxynucleotides (ODNs) containing unmethylated deoxycytidyl-deoxyguanosine (CpG) motifs (CpG-ODN; Krieg, 2002b). TLR9, expressed by B cells, macrophages, and dendritic cells (DCs), recognizes CpG in the acidic environment of the endosome (Ahmad-Nejad et al., 2002). Variant sequences flanking the stimulatory CpG core motif have been described for optimal TLR9 activation expressed by specific cell types. Depending on the cytokines secreted, those ODNs have been categorized as A, B, or C class ODNs; however, it remains unclear why specific CpG sequences trigger different biological effects (Krieg, 2002b).

Studies using fluorescently labeled ODNs indicate that both stimulatory and nonstimulatory ODNs are internalized nonspecifically, but only stimulatory ODNs activate TLR9 in endosomes, where both ligand and receptor colocalize (Hacker et al., 1998; Latz et al., 2004; Leifer et al., 2004; Takeda and Akira, 2005). Uptake of ODN is dependent on dose, time, and temperature but independent of the CpG motif (Guo and Schluesener, 2004).

Upon recognition of CpG-rich sequences in the endosome, TLR9 initiates a conserved TLR family signaling cascade

THE JOURNAL OF CELL BIOLOGY

that begins with the recruitment of the adaptor protein MyD88 via the Toll/interleukin (IL) 1 receptor domain (Ahmad-Nejad et al., 2002). MyD88 then recruits IL-1 receptor–associated kinase (IRAK) 1 and 4 (Wesche et al., 1997). When phosphorylated by IRAK-4, IRAK-1 interacts with TRAF6 (TNF receptor–associated factor 6; Cao et al., 1996; Li et al., 2002) and disengages from the receptor. A complex consisting of TRAF6, TAK1 (TGFβ-activated kinase 1), and TAB (TAK1 binding protein) 1 and 2 goes on to activate the IκB kinase complex, resulting in nuclear factor (NF) κB translocation to the nucleus (Mercurio et al., 1997; Regnier et al., 1997; Jiang et al., 2003). CpG-induced NF-κB activation initiates the up-regulation of costimulatory molecules and the secretion of proinflammatory cytokines, such as TNFα and IL-6.

The adaptor protein MyD88 plays a crucial role in transducing signals from TLR family members. Upon binding to TLR4, bacterial lipopolysaccharide not only activates NF-κB via the MyD88–IRAK serine/threonine kinase pathway but also induces tyrosine phosphorylation in macrophages (Weinstein et al., 1991). Two Src family kinases (SFKs), Hck and Lyn, are responsible for initiating this pathway (English et al., 1993; Beaty et al., 1994). Hck has been shown to regulate differentiation and several actin-dependent processes such as F-actin–based membrane protrusions (Carreno et al., 2002), monocyte chemotaxis (Resnati et al., 1996; Chiaradonna et al., 1999), phagocytosis (Suzuki et al., 2000; Le Cabec et al., 2002), and cellular adhesion (Suen et al., 1999; Scholz et al., 2000). In the well-characterized system of Fcγ receptor signaling, Hck and Lyn are the initiating tyrosine kinases that phosphorylate immunoreceptor tyrosine-based activation motifs (ITAMs) in the signaling chains of the receptor complex, which then serve as docking sites for a second tier of tyrosine kinases such as Syk (Bolen and Brugge, 1997). Both Src and Syk family kinases phosphorylate several downstream signaling
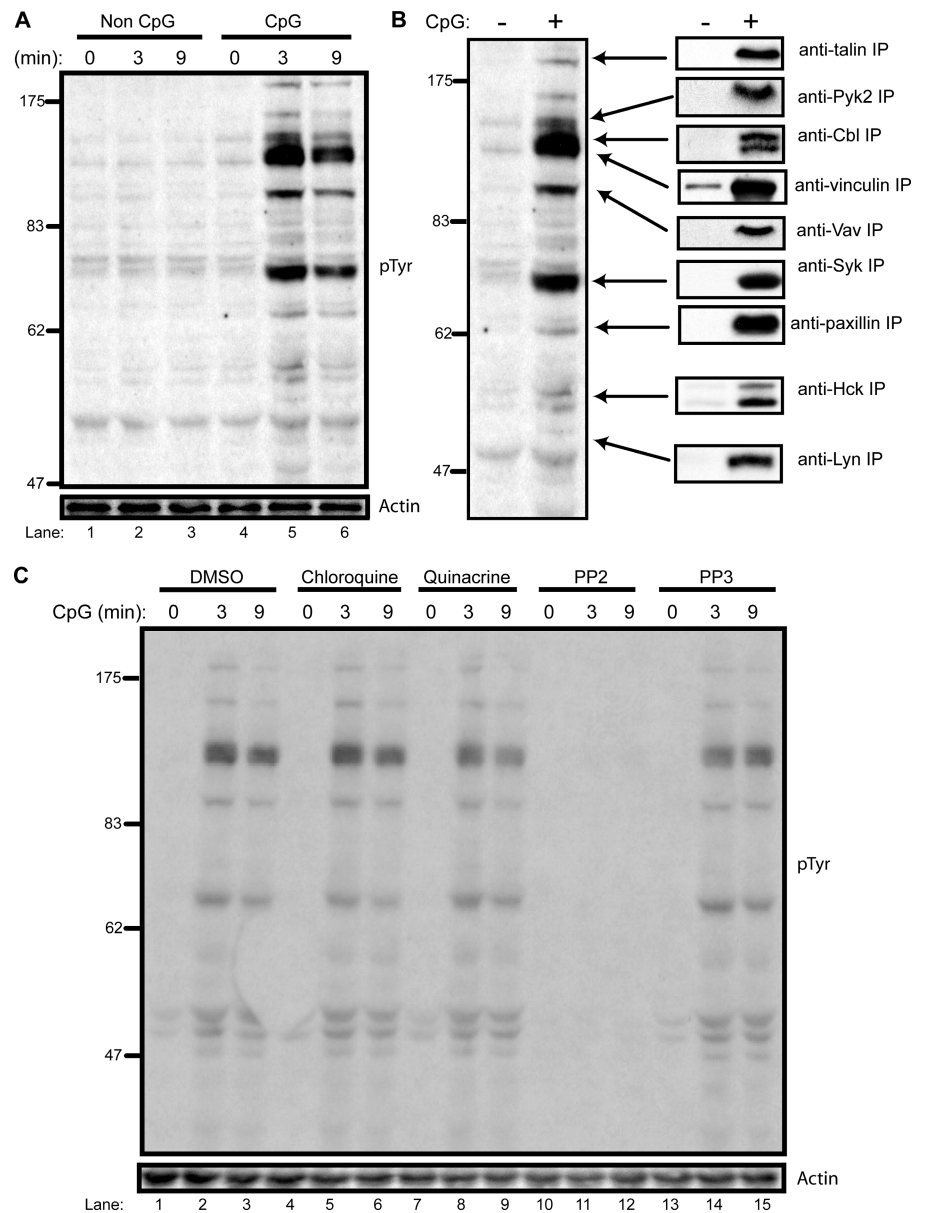

Figure 1. **SFKs initiate a chloroquine-insensitive, CpG-triggered tyrosine phosphorylation cascade.** (A) THP-1 monocytes were stimulated with a control ODN, GpC (lanes 1–3), and CpG–ODN 2216 (lanes 4–6) at 1 μg/ml for the indicated times. 50-μg aliquots of lysate were subjected to SDS-PAGE followed by immunoblotting with an anti-pTyr antibody. Loading controls were immunoblotted with an anti-actin antibody. (B) Individual phosphoproteins were immunoprecipitated with the indicated antibodies from 100 μg of GpC- or CpG-stimulated (3 min) cell lysate and then immunoblotted with anti-pTyr antibody. (C) THP-1 cells were pretreated for 30 min with vehicle (lanes 1–3), 10 μM chloroquine (lanes 4–6), 1 μM quinacrine (lanes 7–9), 1 μM of the SFK inhibitor PP2 (lanes 10–13), and 1 μM of the control inhibitor PP3 (lanes 13–15). Lysates were prepared after CpG stimulation and immunoblotted with anti-pTyr antibody.

proteins and thus initiate multiple signaling events. It has recently been reported that CpG-ODN stimulation induces tyrosine phosphorylation of the GTP exchange factor Vav1 (Stovall et al., 2004).

The TLR9 inhibitor chloroquine and analogues such as quinacrine inhibit immune stimulation by bacterial DNA and CpG-ODN (Macfarlane and Manzel, 1998; Strekowski et al., 1999). The inhibition of TLR9 occurs at endosomes where chloroquine was shown to block CpG and TLR9 interaction (Rutz et al., 2004). Chloroquine (Trape et al., 2002) has also proven effective in the treatment of inflammatory diseases such as systemic lupus erythematosus and rheumatoid arthritis (Fox et al., 1987; Wallace, 2001; Araiza-Casillas et al., 2004; Nord et al., 2004).

We have investigated the role of SFKs upon CpG-induced TLR9 stimulation. Two SFKs, Hck and Lyn, are phosphorylated upon monocyte stimulation with CpG-ODN but not when cells are treated with nonstimulatory deoxyguanosine-deoxycytidyl (GpC) ODN. The SFK-initiated tyrosine phosphorylation cascade activates signaling proteins implicated in reorganization of the actin cytoskeleton, resulting in cell spreading, adhesion, and motility. Surprisingly, the TLR9 inhibitor chloroquine failed to block SFK activation and any of the signaling pathways downstream of tyrosine kinase activation. Macrophages from TLR9$^{-/-}$ and MyD88$^{-/-}$ mice exhibited normal SFK activation, indicating that the SFK pathway is TLR9 independent. Unexpectedly, this pathway is triggered upstream of the traditional TLR9 pathway, as indicated by SFK inhibitors, which blocked CpG-induced phosphorylation of the NF-κB regulator IκB, IL-6 secretion, and up-regulation of CD40 and CD69. Both pathways intersect at the level of TLR9, which is tyrosine phosphorylated upon CpG stimulation and interacts with the tyrosine kinase Syk. Furthermore, CpG-coated beads induce strong actin polymerization at the plasma membrane–bead contact area of macrophages in a chloroquine-insensitive manner. Together, these findings indicate that the SFK-driven tyrosine phosphorylation pathway is an early CpG-induced event that is initiated at the cell surface and is upstream of and required for TLR9/MyD88 activation in endosomes.

Results

CpG induces SFK activation

The role of SFKs after CpG-ODN treatment is unclear. To study the role of tyrosine kinases in TLR9 signaling, we stimulated the human monocyte cell line THP-1 with a control GpC and an activating CpG-ODN. Cell lysates were then analyzed by immunoblotting with an anti-phosphotyrosine (pTyr) antibody. CpG treatment induced rapid tyrosine phosphorylation of multiple proteins, with maximum phosphorylation achieved 3 min after stimulation (Fig. 1 A, lanes 4–6). The control non–CpG-ODN did not trigger tyrosine kinase activation (Fig. 1 A, lanes 1–3).

To specifically identify phosphoproteins, candidate proteins were immunoprecipitated and then immunoblotted with anti-pTyr antibody. Major phosphoproteins of 47, 52, 70, 95, 120, and 125 kD were identified in this manner (Fig. 1 B). The three most prominent phosphoproteins identified were the cytoplasmic tyrosine kinase Syk (70 kD), the hematopoietic-specific exchange factor Vav1 (95 kD), and the adaptor protein Cbl (120 kD). Two SFK members expressed in monocytic cells, Lyn (49 kD) and Hck (52 kD), were also phosphorylated upon CpG treatment. In addition, the hematopoietic-specific focal adhesion kinase Pyk2 (125 kD), talin (200 kD), paxillin (68 kD), and vinculin (117 kD) were also phosphorylated. However, other prominent B cell and macrophage tyrosine substrates, such as B cell linker protein and Bruton's tyrosine kinase, were not phosphorylated upon CpG stimulation (unpublished data).

CpG-induced tyrosine phosphorylation is Src-kinase dependent but chloroquine insensitive

Because our results indicated that two SFKs, Hck and Lyn, were phosphorylated upon CpG treatment, we wanted to test whether an SFK inhibitor could block tyrosine phosphorylation. Pretreatment of THP-1 cells with PP2, a potent SFK inhibitor, completely blocked CpG-induced phosphorylation (Fig. 1 C, lanes 10–12). Pretreatment with PP3, an inactive version of PP2, had no effect on CpG-induced tyrosine phosphorylation (Fig. 1 C, lanes 13–15). Pretreatment with two well-described inhibitors of TLR9-induced cytokine production, chloroquine
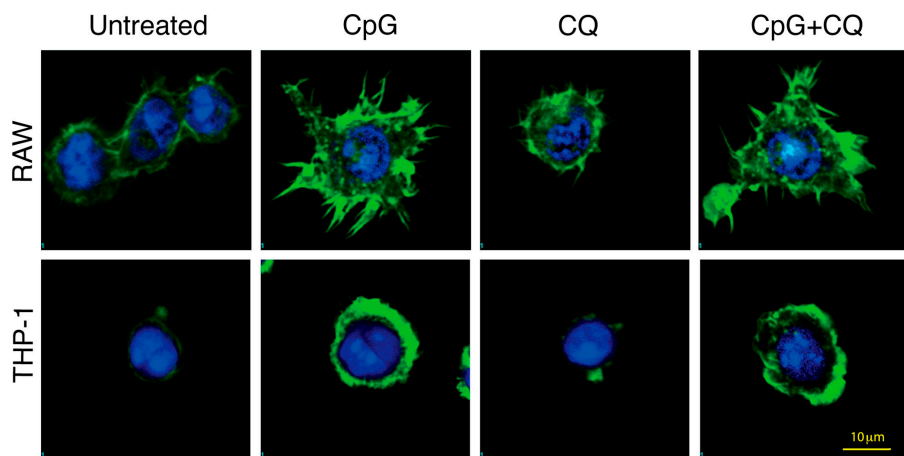

Figure 2. **Chloroquine fails to block CpG-induced actin polymerization.** Mouse macrophages (RAW) or human monocytes (THP-1) were pretreated for 15 min with 10 μM chloroquine (CQ) or vehicle control and then stimulated for 20 min with 1 μg/ml of the mouse-selective CpG–ODN 1668 or human CpG–ODN 2216, respectively. After fixation, cells were stained with FITC-phalloidin (green) and nuclei were visualized with TOPRO-3 (blue).

Figure 3. **CpG-induced cell adhesion is insensitive to chloroquine but requires SFK activity.** (A) Cells were stimulated with 1 μg/ml of a control GpC-ODN or with CpG–ODN 2216 for the indicated times (min). After fixation, cells were visualized as described in Materials and methods. (B) THP-1 cells were preincubated for 10 min with chloroquine, quinacrine, PP2, and PP3. The number at the lower right corner of each panel indicates the concentration for each inhibitor used (μM). Cells were then stimulated for 30 min with CpG, and adhesion was measured. Representative fields are presented. (C) THP-1 cells were stimulated as indicated in A, and images captured from 36 different fields from at least four different wells were quantified to obtain cell number per field and plotted with the SD. (D) THP-1 cells were stimulated for 20 min with increasing concentrations of CpG, control GpC, the B class oligo 2006 (ODN 2006), and murine CpG (mCpG), and adhesion was measured. (E) Adhesion was measured on THP-1 cells that were pretreated for 10 min with increasing concentrations of PP2, PP3, and herbimycin A and then stimulated with CpG for 30 min. Data are represented as percentage of adhered cells versus vehicle-pretreated cells. (F) THP-1 cells were preincubated for 10 min with increasing concentrations of chloroquine or quinacrine. Cells were then stimulated for 30 min with CpG, and the number of adhered cells from at least 36 different fields was quantified. Error bars indicate SD.
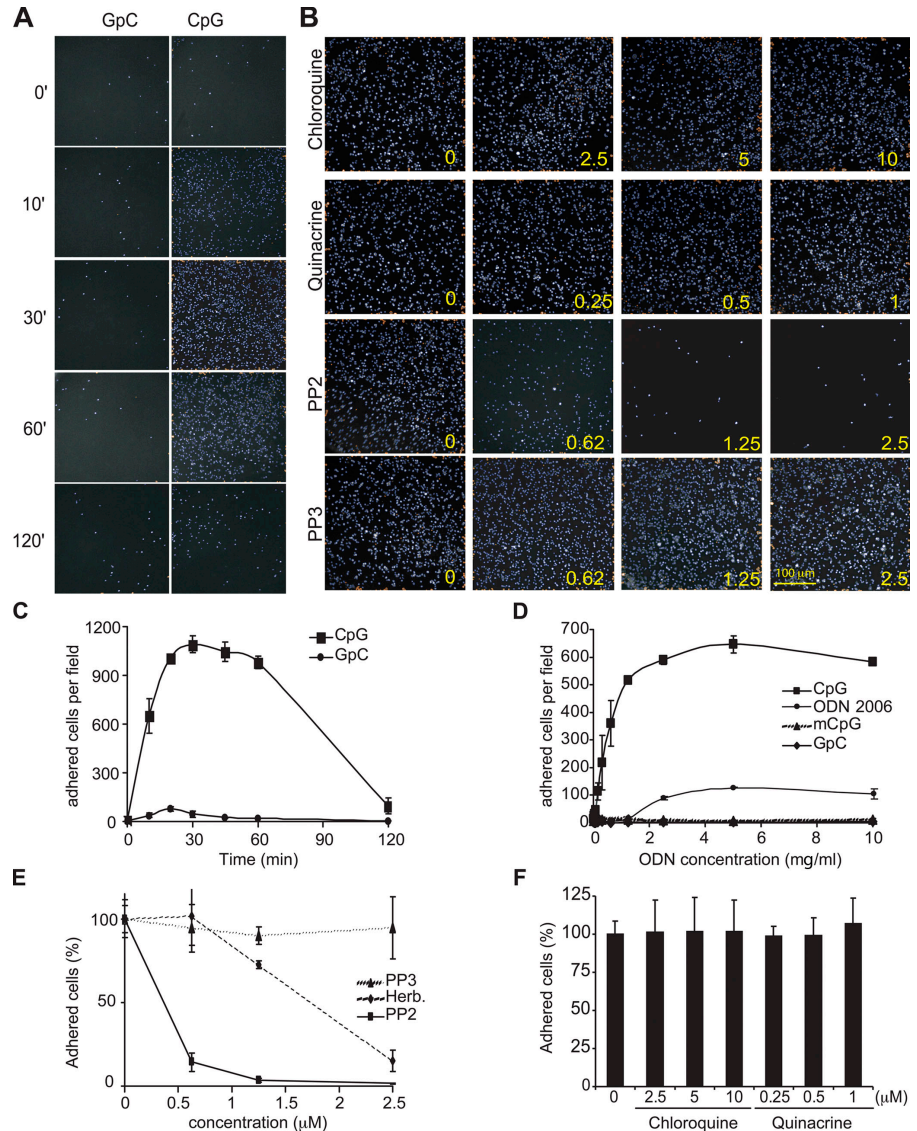
and quinacrine, also had no effect on CpG-induced tyrosine phosphorylation (Fig. 1 C, lanes 4–9).

CpG-induced actin cytoskeleton reorganization is chloroquine insensitive

SFK activation results in cytoskeleton changes and the transcription of effector genes (Latour and Veillette, 2001). Six of the proteins that we found to be phosphorylated upon CpG stimulation, Pyk2, Vav, Cbl, talin, paxillin, and vinculin, along with the activation of PI3K, have been described as mediators of actin cytoskeleton reorganization (Suen et al., 1999; Caveggion et al., 2003; Chodniewicz and Zhelev, 2003; Tybulewicz et al., 2003; Nayal et al., 2004; Mitra et al., 2005). These events promote cell spreading, adhesion, and motility, resulting in monocyte recruitment to areas of infection. When cells were stained for F-actin fibers, we found that CpG treatment induced strong actin polymerization in both mouse macrophages and human monocytes (Fig. 2). These rearrangements translated to rapid cell spreading, conspicuous morphological changes, and increased cell size. In the case of THP-1 cells, CpG treatment

induced the formation of actin-rich lamellipodia structures. Similar to CpG-induced tyrosine kinase phosphorylation (Fig. 1), the TLR9 inhibitor chloroquine was unable to block CpG-induced actin reorganization (Fig. 2).

CpG induces the transient adhesion of monocytes

SFK-initiated actin reorganization can also facilitate cell adhesion to promote the recruitment of cells to tissues infected by pathogens. Because CpG induced cytoskeleton reorganization, we next tested the ability of CpG to induce monocyte adhesion. When human monocytes were stimulated with CpG, they rapidly adhered in culture, with maximal adhesion detected at 30 min (Fig. 3, A and C). A negative control GpC-ODN failed to induce monocyte adhesion. Interestingly, a time-course analysis of CpG-induced adhesion indicated that this event was transient, with cells detaching after 2 h (Fig. 3, A and C). Overnight culture of CpG-stimulated monocytes revealed that cells eventually reattach, an event that we hypothesize is driven by secondary CpG-induced effects, such as

chemokine secretion, because it can be blocked by chloroquine (unpublished data).

Next, we further characterized the ability of different CpG-ODNs to induce adhesion. We found that the human CpG-ODN that induced robust tyrosine phosphorylation also induced adhesion in a concentration-dependent manner (Fig. 3 D). Although 2 μg/ml CpG produced the highest level of adhesion, 0.5 μg/ml was sufficient to induce significant adhesion (Fig. 3 D). A GpC control ODN or a mouse-selective CpG-ODN was unable to induce significant cell adhesion at any concentration tested. Interestingly, when we compared the performance of an A class ODN with that of a B class ODN (ODN 2006), we found that the latter yielded a less pronounced adhesion response (Fig. 3 D). This also correlated with a poor induction of the tyrosine phosphorylation cascade (unpublished data). Although only immunostimulatory CpG promotes cytoskeleton rearrangement, it has been reported that both immunostimulatory and nonimmunostimulatory ODNs are internalized at the same rate in a time-, dose-, and temperature-dependent manner (Hacker et al., 1998; Guo and Schluesener, 2004; Takeda and Akira, 2005; unpublished data), indicating that CpG-induced SFK activation does not enhance ODN uptake. This is consistent with our observations that PP2 treatment had no effect on CpG internalization (unpublished data).

Our previous experiments indicated that inhibition of SFKs blocked the phosphorylation of proteins that promote cellular adhesion, such as Pyk2 and Vav1 (Fig. 1). Based on these data, we hypothesized that the SFK inhibitor PP2 would also block monocyte adhesion. When we tested this hypothesis, we found that PP2 potently blocked CpG-induced adhesion, even at concentrations below the micromolar range (Fig. 3, B and E). As expected, the control inhibitor PP3 had no effect on monocyte adhesion. Herbimycin A, another SFK inhibitor, also blocked monocyte adhesion at submicromolar concentrations (Fig. 3 E). Actin-driven morphological changes are dynamic processes mediated by the polymerization and depolymerization of actin fibers. Therefore, we examined the effects of the actin microfilament–disrupting drugs cytochalasin D, latrunculin A, and jasplakinolide. All three inhibitors potently blocked monocyte adhesion at the nanomolar range (Fig. S1, available at http://www.jcb.org/cgi/content/full/jcb.200508058/DC1). Together, these data indicated that CpG-triggered SFK activation initiates a tyrosine-kinase signaling cascade in monocytes that results in actin-driven cytoskeleton changes that promote cell adhesion.

SFK-dependent cellular responses are chloroquine insensitive

Chloroquine blocks CpG interaction with TLR9 at the endosome (Rutz et al., 2004), and our previous findings indicated that although CpG-induced tyrosine kinase activation was blocked by the SFK inhibitor PP2, it was insensitive to chloroquine (Fig. 1 C). We therefore tested the ability of chloroquine and quinacrine to modulate CpG-induced adhesion. Even at high concentrations that completely inhibit TLR9-induced cytokine production (10 μM for chloroquine and 1 μM for quinacrine), both inhibitors failed to block CpG-induced adhesion (Fig. 3, B and F).
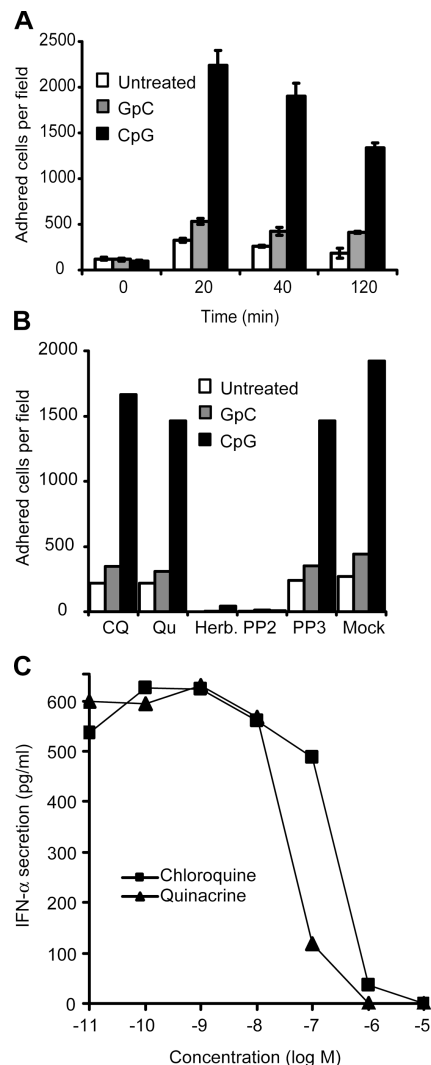
Figure 4. **CpG-induced chloroquine-insensitive adhesion of human DCs.** (A) Adhesion was measured in human monocyte–derived immature DCs, as described in Fig. 3. Cells were stimulated with CpG–ODN 2216, and the number of adhered cells was obtained at the indicated times. White bars represent background adhesion, gray bars indicate adhesion in the presence of a control GpC-ODN, and black bars indicate adhesion induced by CpG-ODN. Error bars indicate SD. (B) DCs were preincubated for 15 min with chloroquine (CQ; 10 μM), quinacrine (Qu; 1 μM), herbimycin A (5 μM), PP2 (1 μM), and PP3 (1 μM). Cells were then stimulated with GpC and CpG-ODN, and adhesion was quantified as previously described. (C) pDCs purified from human PBMCs were incubated with the indicated concentrations of chloroquine and quinacrine in the presence of CpG for 18 h. Culture supernatants were analyzed for secreted IFN-α by ELISA.

To corroborate our findings using primary cells, we repeated these studies using immature human DCs. Similar to a human monocytic cell line, CpG induced adhesion of human monocyte–derived DCs, whereas GpC did not (Fig. 4 A). In immature DCs, we found that SFK inhibitors are able to effectively block CpG-induced adhesion (Fig. 4 B). Although chloroquine and quinacrine blocked IFN-α secretion from peripheral blood mononuclear cells (PBMCs) at concentrations of <10 and 1 μM, respectively (Fig. 4 C), they were unable to block CpG-induced adhesion at similar concentrations (Fig. 4 B).
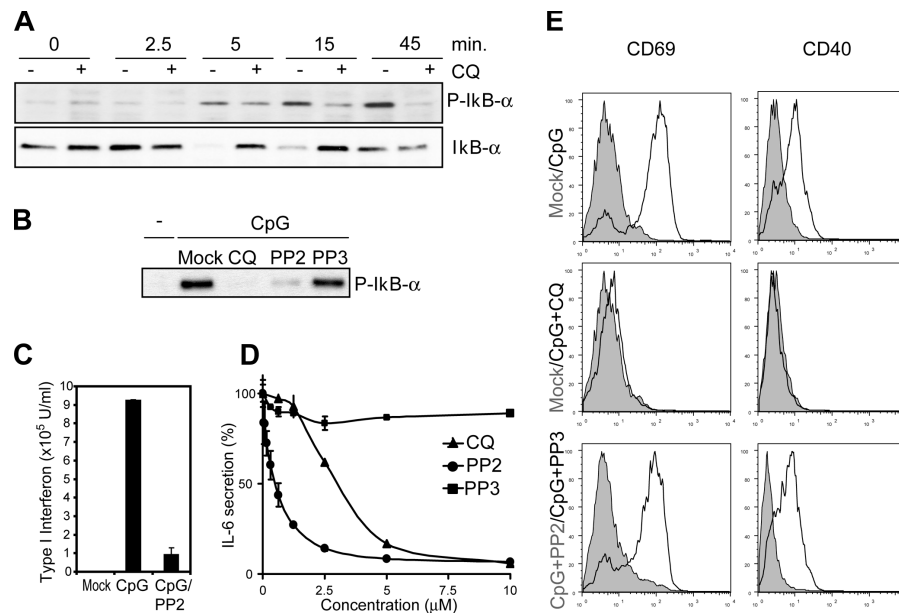
Figure 5. **CpG-induced SFK activation is upstream of NF-κB activation.** (A) Raw cells lysates were collected after CpG treatment (ODN 1585) in the presence or absence of 10 μM chloroquine (CQ). IκB-α was immunoprecipitated, and the product was resolved by SDS-PAGE and immunoblotted with a phospho–IκB-α antibody. The degradation of IκB-α was also detected using an IκB-α antibody. (B) Cells were pretreated with the SFK inhibitor PP2 and its control PP3. Lysates were analyzed as described in A. (C) Isolated pDCs from human blood were cultured for 18 h and then preincubated for 15 min with vehicle or PP2 (2 μM). Cells were then stimulated with 5 μM CpG. After 24 h of culture, supernatants were taken and analyzed for type I interferon levels. (D) Splenocytes from B6 mice were pretreated for 1 h with increasing concentrations of PP2, PP3, and chloroquine and then stimulated with CpG for 12 h. Supernatants were analyzed for IL-6 secretion by ELISA. Error bars indicate SD. (E) Splenocytes from D were analyzed for CpG-induced up-regulation of CD69 and CD40 by FACS. Unshaded versus shaded histogram for each panel represents the following: untreated versus CpG stimulated (top), and untreated versus CpG plus chloroquine treatment (middle). (bottom) B cells pretreated with PP2 (unshaded) versus PP3 (shaded) after CpG treatment.

Another prominent cytoskeleton-dependent process is cell motility. All of the identified CpG-induced phosphoproteins have been implicated in driving or regulating cell motility (Fig. 1 B). As previously described (Baek et al., 2001), we found that monocytes migrate toward a CpG gradient (Fig. S2, available at http://www.jcb.org/cgi/content/full/jcb.200508058/DC1). As in the case of adhesion, chloroquine and quinacrine failed to block monocyte migration in response to CpG (Fig. S2).

CpG-triggered SFK activation is required for cytokine secretion

The secretion of CpG-induced inflammatory cytokines is dependent on NF-κB translocation to the nucleus (Krieg, 2002b). The negative regulator of NF-κB activation, IκB-α, is phosphorylated and degraded after 5 min and remains strongly phosphorylated 45 min after CpG treatment (Fig. 5 A). As expected, the TLR9 inhibitor chloroquine blocked IκB-α phosphorylation and degradation in monocytes (Fig. 5 A). Our previous results (Fig. 1) indicated that CpG-induced SFK activation precedes IκB-α phosphorylation and degradation, which are undetectable at 2.5 min as compared with maximal CpG-induced tyrosine phosphorylation at 3 min after CpG treatment. Given the rapid kinetics of SFK activation and insensitivity to chloroquine treatment, we hypothesized that CpG-induced tyrosine phosphorylation is upstream of IκB-α phosphorylation. When we tested this hypothesis in macrophages, we found that the SFK inhibitor PP2 effectively blocked IκB-α phosphorylation upon CpG stimulation (Fig. 5 B). Like chloroquine, the SFK inhibitor

PP2 also inhibited CpG-induced IFN-α secretion in immature human plasmacytoid DCs (pDCs; Fig. 5 C). Furthermore, PP2 effectively blocked CpG-induced IL-6 secretion (Fig. 5 D) and the up-regulation of B cell activation markers such as CD40 and CD69 (Fig. 5 E). To complement our pharmacological inhibitor data, we established a small interfering RNA (siRNA) system to specifically knock down the expression of Lyn and Hck, two leukocyte SFKs that we identified as being activated by CpG. Immunoblot analysis of siRNA-transfected cell lysates revealed that an 80% knockdown of Lyn and a >90% knockdown of Hck was achieved (Fig. 6 A). When these cells were used in a CpG-induced adhesion assay, single knockdown of Lyn or Hck resulted in a significant decrease in cellular adhesion (Fig. 6 B). A combined knockdown of Lyn and Hck further decreased CpG-induced adhesion by ∼60%. The residual adhesion is most probably mediated by other SFKs, such as Blk, Fyn, and Src. Moreover, analysis of cytokine production revealed a similar trend, where combined knockdown of Lyn and Hck reduced CpG-induced TNFα production by ∼60% (Fig. 6 C). Together, both the pharmacological inhibitor and genetic data indicated that early activation of SFKs plays a key role in CpG-induced activation of monocytes.

CpG-triggered SFK activation is upstream of MyD88 and originates at the plasma membrane

The SFK pathway remains intact even when the TLR9– MyD88 signaling pathway is blocked using chloroquine. Next, we used
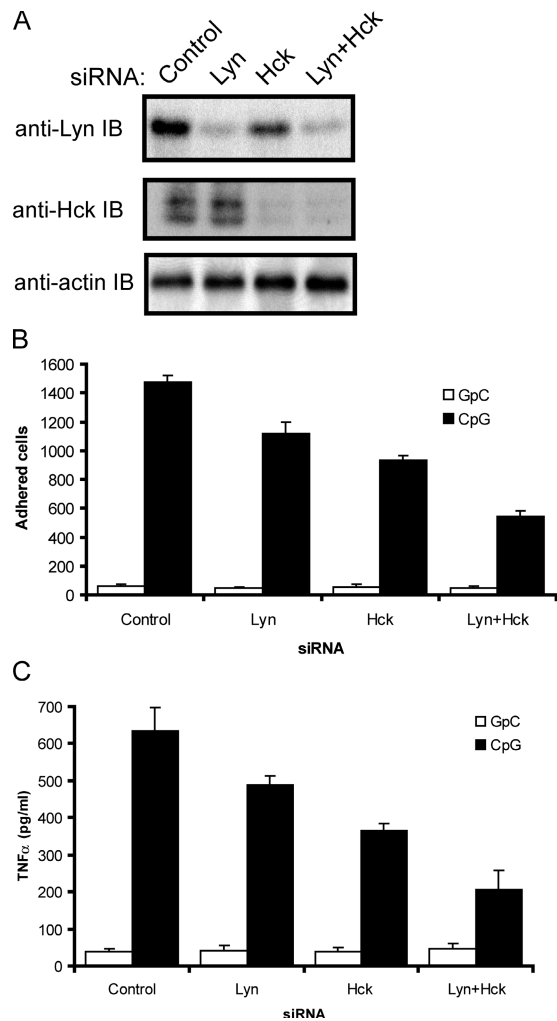
A

B

C

Figure 6. **Knockdown of SFK expression by siRNA significantly inhibits CpG-induced adhesion and cytokine production.** (A) THP-1 cells were transfected with control-scrambled siRNA or siRNA pools for Lyn, Hck, or both kinases and then cultured for 48 h. Gene knockdown was visualized by immunoblotting lysates with anti-Lyn or anti-Hck antibodies. (B) Cells from A were stimulated with GpC control or CpG–ODN 2216 (1 μM) for 20 min and tested in an adhesion assay, as described in Fig. 3 A. (C) THP-1 cells from A were plated at 5×10^5 cells/well in triplicate. Cells were stimulated with a GpC control or CpG–ODN 2216 for 4 h. TNFα in culture supernatants was measured by ELISA. Error bars indicate SD.

A

B

C

Figure 7. **CpG activates SFKs at the plasma membrane and upstream of the MyD88 activation.** (A) Thioglycollate-elicited peritoneal macrophages were obtained from wild-type and MyD88$^{-/-}$ mice and cultured for 24 h in medium containing 0.5% FBS. Cells were pretreated with 10 μM chloroquine (CQ) or vehicle for 15 min and stimulated with CpG–ODN 1585 for 5 min. Tyrosine phosphorylation after CpG treatment was visualized by immunoblotting with an anti-pTyr antibody. (B) Murine bone marrow–derived DCs from wild-type and MyD88$^{-/-}$ mice were pretreated with 10 μM chloroquine or vehicle for 15 min, and after CpG stimulation, cells were stained with an antibody to the p65 subunit of NF-κB. (C) CpG- or GpC-coated 10-μm red fluorescent polystyrene beads were added to RAW cells for 20 min. Cells were then fixed and stained with FITC-phalloidin. The yellow arrow indicates the location of cells.

an alternative method to pharmacological inhibitors to confirm our results. Because the adaptor protein MyD88 is required for signal transduction downstream of TLR9, we decided to test whether the CpG-induced tyrosine phosphorylation cascade is intact in the absence of MyD88. The same intensity and kinetics of phosphorylation was observed in both control and MyD88$^{-/-}$ macrophages stimulated with CpG-ODN (Fig. 7 A). Consistent with our previous results, chloroquine treatment did not block CpG-induced tyrosine phosphorylation in either wild-type or MyD88$^{-/-}$ macrophages (Fig. 7 A). Although the SFK pathway was intact in MyD88$^{-/-}$ macrophages, CpG treatment was unable to induce translocation of the p65 subunit of NF-κB to the nucleus (Fig. 7 B). Consequently, NF-κB–driven responses such as the up-regulation of CD40 and CD69 and the secretion of IL-6
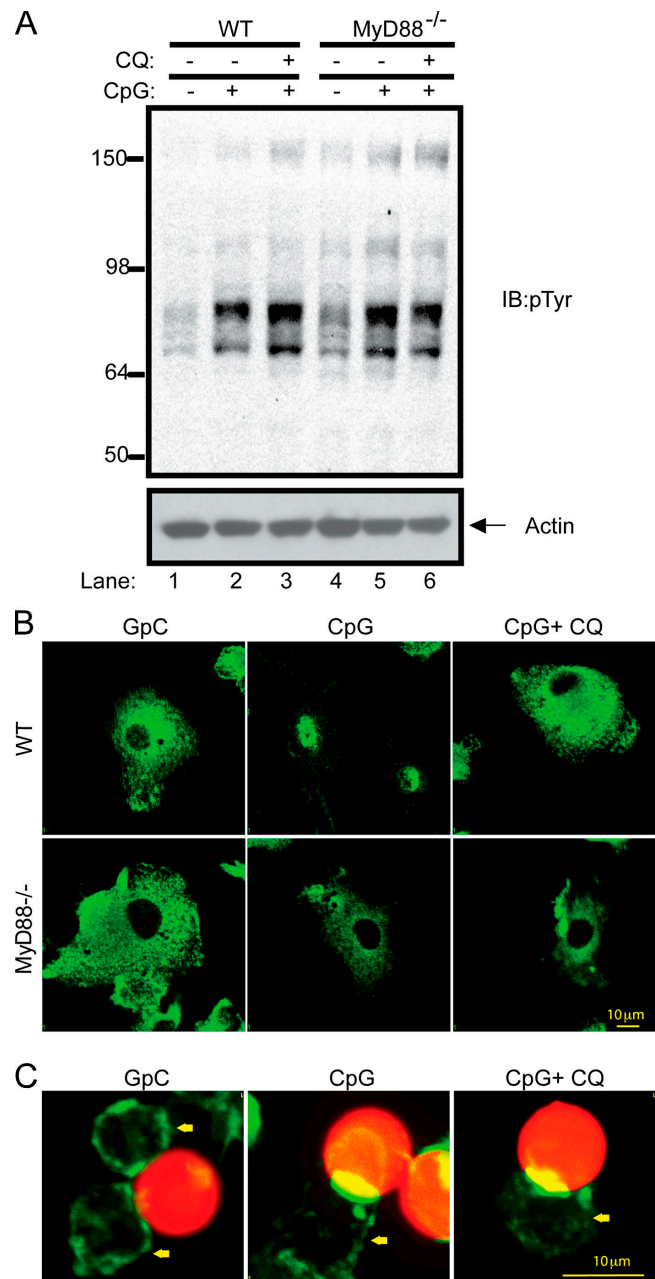
were impaired in cells from MyD88$^{-/-}$ mice (Fig. S3, available at http://www.jcb.org/cgi/content/full/jcb.200508058/DC1).

Because our data indicated that the SFK pathway was activated at the cell surface, we decided to directly test this

Figure 8. CpG-induced SFK activation is a TLR9-independent event. (A) Thioglycollate-elicited peritoneal macrophages were obtained from wild-type (WT) and TLR9−/− mice. After 24 h of culture in medium (0.5% FCS), cells were stimulated with CpG–ODN 1585 for 5 and 10 min. Tyrosine phosphorylation after CpG treatment was visualized by immunoblotting with an anti-pTyr antibody. (B) Peritoneal macrophages obtained from wild-type, MyD88−/−, and TLR9−/− mice were cultured for 24 h, and CpG- or GpC-coated 15-μm red fluorescent polystyrene beads were added for 20 min. Cells were then fixed and stained with FITC-phalloidin. (C) High-binding 96-well plates were coated with 100 μl of a CpG solution for 15 h at 0.5 and 1 μg/ml, and unbounded ODN were removed by washing thoroughly. Peritoneal macrophages were plated at 2×10^5 cells per well. A different group of cells was stimulated with soluble CpG at the indicated concentration. 15 h later, supernatants were collected and secreted IL-6 was measured by ELISA. (D) Freshly isolated peritoneal macrophages were allowed to attach for only 10 min to wells previously covered with CpG and GpC. After paraformaldehyde fixation, cells were stained with FITC-phalloidin (green) and nuclei were visualized with TOPRO-3 (red). (E) Adhesion was assayed in THP-1 cells pretreated with wortmannin at increasing concentrations, as previously described. (F) THP-1 cells were pretreated with 10 μM chloroquine (CQ), 1 μM PP2, and 1 μM wortmannin (W) for 20 min. After CpG stimulation for 5 min, the phosphorylation of Akt was analyzed by Western blot. (G) THP-1 cells expressing Flag-TLR9 were pretreated with 10 μM chloroquine and 1 μM PP2 for 20 min. After stimulating the cells for 5 min, samples were lysed and TLR9 was immunoprecipitated using an anti-Flag antibody. Flag-TLR9 and Syk were then detected by Western blot. (H) Cells were pretreated as before and also with Syk inhibitor (SI). Immunoprecipitated TLR9 was assayed with anti-pTyr (4G10).
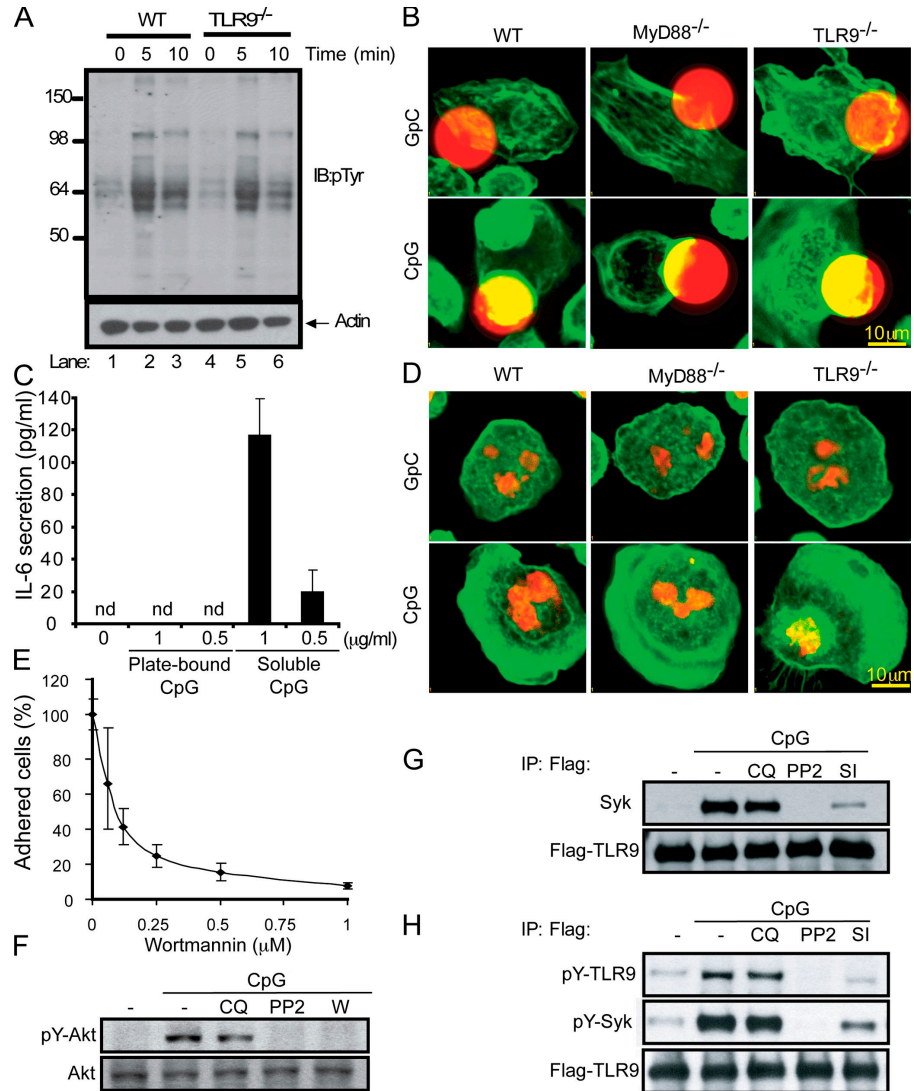
hypothesis by stimulating cells with CpG-ODN that are unable to be internalized. 10-μm red fluorescent polystyrene beads that are large enough to avoid internalization by macrophages were coated with CpG or control GpC-ODN. Upon incubating these beads with mouse macrophages for 20 min, we observed strong actin polymerization localized specifically at the plasma membrane of the cell–bead contact area (Fig. 7 C). Beads coated with CpG, but not with the control GpC-ODN, specifically induced this actin polymerization. Consistent with our previous findings, actin reorganization was chloroquine insensitive (Fig. 7 C).

The SFK pathway is TLR9 independent but intersects with the MyD88 pathway

It has recently been reported that CpG-induced Akt phosphorylation occurs via a TLR9-independent pathway (Dragoi et al., 2005). It is possible that the chloroquine-insensitive SFK pathway that we describe originates at the plasma membrane in a TLR9-independent manner, similar to that described for Akt phosphorylation. Once CpG is internalized into endosomes, it would interact with TLR9 and initiate the chloroquine-sensitive TLR9–MyD88 pathway. To test this hypothesis, we stimulated TLR9−/− macrophages with CpG and obtained a pattern of tyrosine phosphorylated proteins similar to that of wild-type macrophages, indicating that CpG-induced SFK activation is intact in cells lacking TLR9 (Fig. 8 A). Furthermore, the downstream actin cytoskeleton rearrangements were also unperturbed in cells from both TLR9−/− and MyD88−/− mice stimulated with CpG-coated beads (Fig. 8 B). These data indicate that this pathway is both TLR9 independent and initiated at the cell surface before CpG endocytosis. Although CpG recognition can happen before CpG internalization, as we show here, it has been demonstrated that CpG internalization is required for cell activation and cytokine production (Krieg et al., 1995; Manzel and Macfarlane, 1999; Ahmad-Nejad et al., 2002). In accordance with these findings, plate-bound CpG was unable to induce IL-6 secretion (Fig. 8 C). Although the TLR9–MyD88 pathway was impaired when CpG was immobilized, confocal analyses indicated that CpG-induced cytoskeletal rearrangements were intact (Fig. 8 D). Macrophages stimulated with CpG immobilized on plastic generated large, actin-rich lamellipodia. Similar actin rearrangements were observed in macrophages from MyD88−/− and TLR9−/− mice (Fig. 8 D).

Next, we examined whether the CpG-induced SFK pathway is upstream of the previously described TLR9-independent phosphorylation of Akt (Dragoi et al., 2005). Activation of SFKs promotes actin reorganization through the participation of PI3K, an upstream regulator of Akt (Franke et al., 1997). Treatment of cells with the PI3K inhibitor wortmannin inhibited both CpG-induced cell adhesion (Fig. 8 E) and phosphorylation of Akt (Fig. 8 F). Furthermore, use of the SFK inhibitor PP2 blocked CpG-induced Akt phosphorylation (Fig. 8 F), indicating that the SFK pathway is upstream of the previously reported TLR9-independent phosphorylation of Akt.

Given that the CpG-induced SFK pathway originates at the plasma membrane and TLR9 is itself located in endosomes, we next wanted to investigate how these two pathways intersect. Recently, Syk, a CpG-activated kinase that we identified (Fig. 1), was reported to be a key component in the innate response to zymosan (Rogers et al., 2005). Syk was shown to couple to the β-glucan receptor Dectin-1 and work synergistically with TLR2 to mount an immune response to zymosan. Using a THP-1 cell line expressing a Flag-tagged TLR9, we found that upon CpG stimulation Syk coimmunoprecipitates with TLR9 (Fig. 8 G). This interaction provides a link between the SFK pathway and the MyD88 pathway. This interaction is unperturbed in the presence of the TLR9 inhibitor chloroquine, suggesting that it occurs before the generation of a signal through TLR9. Both the SFK inhibitor PP2 and a specific Syk inhibitor blocked the interaction of Syk with TLR9. To further examine the association of Syk with TLR9, we examined whether TLR9 itself was tyrosine phosphorylated. CpG treatment did indeed induce tyrosine phosphorylation of TLR9 (Fig. 8 H). Consistent with our previous experiments, this event was chloroquine insensitive but completely blocked by PP2 and partially blocked with a Syk inhibitor.

Discussion

CpG-containing ODNs activate TLR9 in endosomes and trigger the secretion of inflammatory cytokines by a mechanism that is dependent on the adaptor protein MyD88 (Krieg, 2002b; Takeda et al., 2003). We demonstrate that cellular activation by immunostimulatory ODNs is more complex than previously described and requires a TLR9-independent SFK-driven pathway. This SFK-dependent signaling cascade is not parallel but upstream of the chloroquine-sensitive TLR9–MyD88 pathway.

We first provide evidence that stimulation with CpG, but not the control GpC, induces a complex pattern of tyrosine phosphorylation in monocytes. While characterizing several of these phosphorylated proteins, we identified two SFKs expressed in myeloid cells, Hck and Lyn. Treatment of monocytes with the SFK inhibitor PP2 inhibited the CpG-induced tyrosine phosphorylation cascade. Interestingly, treatment with chloroquine and quinacrine, two known inhibitors of TLR9 signaling, failed to block tyrosine phosphorylation.

In addition to the kinases Hck and Lyn, we found that CpG also induced the phosphorylation of Pyk2, Cbl, and the previously described CpG-activated Vav (Stovall et al., 2004). These proteins are required for adhesion and migration responses that involve rearrangement of the actin cytoskeleton

(Suzuki et al., 2000; Latour and Veillette, 2001). For example, the phosphorylation of Pyk2 by SFKs, along with the participation of other focal adhesion proteins, promotes actin cytoskeleton rearrangements that induce cell adhesion, spreading, and lamellipodia formation (Suen et al., 1999). Cbl, which interacts with Pyk2, Vav, and SFKs, has been associated with increased motility of macrophages (Caveggion et al., 2003). Vav, a multidomain signal integrator, transduces signals to cytoskeleton-dependent pathways, which include the PI3K pathway and the activation of extracellular signal–regulated kinase and NF-κB (Tybulewicz et al., 2003). The phosphorylation of Pyk2, Cbl, and Vav upon CpG stimulation suggested that actin reorganization plays an important role upon CpG stimulation. Indeed, our experiments confirmed that CpG triggered the reorganization of the actin cytoskeleton, promoting cell adhesion and migration. We found that CpG treatment induced a transient, SFK-dependent cell adhesion in human monocytes but not when cells were stimulated with either control GpC-ODN or a mouse-selective CpG-ODN. Again, the TLR9 inhibitor chloroquine was unable to block CpG-induced adhesion and migration of THP-1 monocytes and adhesion on human monocyte–derived DCs; however, those cellular responses were completely blocked with an SFK inhibitor.

CpG-induced SFK signaling was upstream and required for NF-κB activation and subsequent cytokine secretion. SFK inhibitors blocked CpG-induced secretion of IL-6 in splenocytes, IFN-α production in human pDCs, and the up-regulation of activation markers on murine B cells. Furthermore, we found that SFK activation was intact in MyD88$^{-/-}$ mice, indicating that this pathway is both upstream and independent of MyD88.

The rapid kinetics of tyrosine phosphorylation suggested that this event was initiated at the cell surface and independent of the endosomal localized TLR9. The use of CpG-coated beads, too large to be internalized, revealed that CpG induced robust, rapid actin reorganization at the bead–cell contact area, further suggesting that these events did not require internalization of CpG. The use of TLR9$^{-/-}$ and MyD88$^{-/-}$ monocytes indicated that these cellular events were independent of TLR9 and MyD88 in addition to being chloroquine insensitive. Together, these studies indicated that CpG-induced SFK activation at the plasma membrane drives cytoskeletal reorganization upstream and independently of the TLR9–MyD88 pathway that could result in cell adhesion and migration. In support of our findings, it was recently reported that, upon DNA viral infection of mice, leukocyte recruitment to the liver is not altered in TLR9$^{-/-}$ and MyD88 $^{-/-}$ mice, whereas the secretion of cytokines in vivo was dramatically reduced (Delale et al., 2005).

Our findings indicate that the recognition of CpG-ODN is more complex than previously described, but as reported (Krieg et al., 1995; Manzel and Macfarlane, 1999), this TLR9-independent pathway cannot induce cytokine secretion without ODN internalization. Although plate-bound CpG induced the formation of large lamellipodia in macrophages from wild-type, TLR9$^{-/-}$, and MyD88$^{-/-}$ mice, it was unable to induce IL-6 secretion.

The TLR9 receptor responds differently to the three identified ODN classes (A, B, and C). The mechanism by which
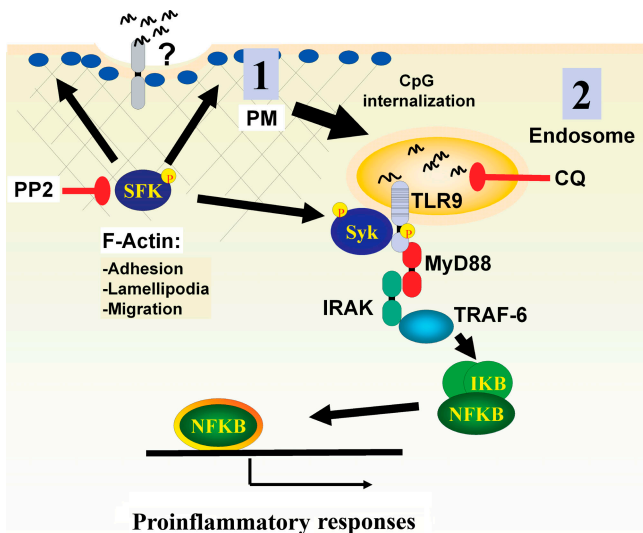
Figure 9. **A model for the two-step activation by CpG-DNA.** We propose that the recognition of A class CpG-DNA is a two-step process that can begin at the plasma membrane (PM) by a TLR9-independent mechanism. We hypothesize the existence of a receptor, localized at the plasma membrane, which is able to distinguish CpG- versus GpC-DNA. CpG-DNA stimulation of this receptor would activate two SFKs, Hck and Lyn, that would initiate a tyrosine phosphorylation cascade that can be fully inhibited with the inhibitor PP2. SFK-mediated actin filament rearrangement is upstream of cell adhesion, spreading, and migration. One downstream effector of the SFK pathway, Syk, interacts with TLR9. The second CpG-induced activation event occurs at the endosome when internalized CpG-DNA binds TLR9 and initiates the MyD88-dependent cascade that is chloroquine sensitive.

these diversified responses are generated remains unresolved (Vollmer et al., 2004). It has been hypothesized that TLR9 requires additional coreceptors/cofactors, as is the case for TLR4 (Verthelyi and Zeuner, 2003), for the recognition of CpG–A class ODNs (Gursel et al., 2002). Our findings support this hypothesis because SFK activation and downstream cellular events are most strongly triggered by CpG–A class ODN when compared with B class ODN. Based on our preliminary characterization of this pathway, we hypothesize that a CpG-sensing coreceptor/cofactor is localized at the plasma membrane, which could also potentially be internalized with CpG-ODN, resulting in endosomal TLR9 activation (Fig. 9). Until this pathway is further characterized, it remains possible that this coreceptor/cofactor is also localized in the endosome in resting cells.

The role of PI3K family on TLR signaling is poorly understood. PI3K interacts with the cytosolic Toll/IL-1 receptor domain of TLR2 (Arbibe et al., 2000) and has been found activated downstream of IRAK1 in response to IL-1β (Neumann et al., 2002). Recently, Akt, a downstream effector of the SFK–PI3K pathway (Franke et al., 1997), was shown to be phosphorylated in response to CpG by a TLR9-independent mechanism that involves DNA-dependent protein kinase (Dragoi et al., 2005). In our experimental system, Akt phosphorylation was intact in chloroquine-treated cells, indicating that the MyD88 cascade is not involved in Akt activation. However, Akt phosphorylation was completely blocked by both PP2 and the PI3K inhibitor wortmannin. These data indicate that the TLR9-

independent tyrosine phosphorylation cascade that we describe is upstream of Akt activation.

Finally, we provide evidence that the SFK pathway does intersect with the TLR9–MyD88 pathway. TLR9 is tyrosine phosphorylated upon CpG stimulation, and this event is independent of chloroquine but blocked by PP2. Furthermore, Syk coimmunoprecipitates with TLR9 upon CpG stimulation, and this interaction can be blocked by PP2. Because Syk is normally recruited to ITAM-containing receptors, which is not the case of TLR9, it is likely that the TLR9–Syk association is indirect and that other proteins participate in the formation of a complex. Two potential ITAM chains, the γ chain of the Fc receptor and DAP12 (DNAX-activating protein of 12 kD) were examined, but no phosphorylation was detected upon CpG stimulation (unpublished data). Although our experiments do not reveal whether Syk associates directly with TLR9, coimmunoprecipitation after CpG stimulation is not affected by chloroquine, indicating that this event is driven by the initial SFK pathway independently of TLR9. This link between tyrosine kinase signaling and TLRs is further supported by a recent study involving TLR3, a receptor for double-stranded RNA. Like TLR9, TLR3 is tyrosine phosphorylated, and this event is linked to PI3K-mediated enhancement of the interferon regulatory factor 3 pathway (Sarkar et al., 2004). Unlike our findings with TLR9, TLR3 phosphorylation does not regulate NF-κB activation.

In conclusion, we describe a TLR9-independent, SFK-driven signaling cascade induced by CpG. This cascade is upstream of the MyD88-dependent endosomal pathway and is initiated at the plasma membrane. This chloroquine-insensitive pathway initiates complex cytoskeletal rearrangements necessary for cell biological events such as adhesion and migration. Moreover, these two pathways interact, as inhibition of the SFK pathway blocks activation events downstream of endosomal TLR9/MyD88 such as NF-κB activation and cytokine secretion. Our findings suggest that a potential CpG-sensing receptor is localized at the plasma membrane and might interact with CpG before the activation of endosomal TLR9. Future studies are required to identify candidate proteins that would perform this function. The identification of a TLR9 coreceptor would potentially provide a new target for pharmaceutical intervention that could result in new treatments for autoimmune diseases.

Materials and methods

Cells
THP-1 and RAW264.7 (RAW) cells were obtained from American Type Culture Collection and cultured in RPMI 1640 medium (Invitrogen) supplemented with 10% FCS (Invitrogen), 2 mM L-glutamine, and antibiotics. Flag-TLR9 stable transfected THP-1 were selected after transfecting THP-1 with NH$_2$-terminal–tagged version of hTLR9 cloned in p3× Flag-CMV-9, where original TLR9 leader peptide was replaced by the one provided in the vector. TLR9$^{-/-}$ and MyD88$^{-/-}$ mice were provided by S. Akira (Osaka University, Suita, Japan). Single-cell spleen suspensions from wild-type (C57BL/6 background) and MyD88$^{-/-}$ mice were obtained after mincing spleens and lysing erythrocytes. Cells were then cultured in RPMI 1640 medium supplemented with 10% FCS. Human monocyte–derived DCs were derived from human peripheral blood as previously described (Vincent et al., 2002). Human pDCs were isolated from PBMC using the BDCA-4 isolation kit (Miltenyi Biotec). Purified pDCs were cultured for 16–20 h in RPMI 1640 supplemented with 10% FCS, GlutaMAX, kanamycin, and Na-pyruvate (all from Invitrogen). IL-3 (R&D Systems) was added to a final

concentration of 20 ng/ml. Unless indicated in the figure legends, type I interferon levels in culture supernatants were measured by evaluating the inhibition of Daudi cell proliferation with reference to a standard IFN-α curve (Nederman et al., 1990).

Murine B cells were obtained by negative selection, removing attached cells and then using anti-Thy1.2 magnetic beads (Dynal). Murine bone marrow–derived DCs were generated from bone marrow progenitors as described by Lutz et al. (1999). In brief, freshly prepared bone marrow cells were cultured in RPMI 1640 medium supplemented with 10% heat-inactivated FCS, 2 mM L-glutamine, 10 mM Hepes buffer, 50 μg/ml penicillin, and nonessential amino acids in the presence of 200 U/ml GM-CSF (granulocyte-macrophage colony-stimulating factor; Sigma-Aldrich). Cultures were supplemented with GM-CSF on days 3 and 8. Murine-elicited macrophages were obtained by peritoneal lavage 4 d after peritoneal injection of 2 ml of thioglycollate broth (Sigma-Aldrich). They were washed three times in FCS-supplemented serum and then plated. 1 h later, unattached cells were discarded. For biochemistry, cells were cultured for 24 h in DME supplemented with 0.5% FCS, 2 mM L-glutamine, 50 ng/ml IFN-γ, and antibiotics and then stimulated as indicated in figure legends.

Antibodies and reagents
Anti-p65, anti–IκB-α, anti-Cbl, anti-Vav, anti-Syk, anti-Syk anti-Hck, and anti-Lyn were obtained from Santa Cruz Biotechnology, Inc. Akt and P-Y-Akt were from Cell Signaling. Monoclonal anti-Flag (M2) was purchased from Sigma-Aldrich. Anti-Pyk2 was purchased from BD Biosciences, and anti-pTyr (clone 4G10), anti-paxillin, anti-vinculin, and anti-talin antibodies were purchased from Upstate Biotechnology. Hoescht 33342, FITC-phalloidin, FluoSpheres polystyrene microspheres (10 μm for RAW cells and 15 μm in diameter for peritoneal macrophages), red fluorescent (580/605), and TOPRO-3 were obtained from Invitrogen. Herbimycin, Syk inhibitor, PP2, and PP3 were purchased from Calbiochem. Chloroquine, quinacrine, lipopolysaccharide, and red blood cell lysis buffer were obtained from Sigma-Aldrich. Oligonucleotides were obtained from GenBase and, unless indicated otherwise, were used at 1 μg/ml. The human stimulatory sequences used were as follows: human ODN2216, referred to as CpG gggggACGATCGTCggggg, and a control ODN, GpC gggggAGCAT-GCTggggg. We used the B class CpG oligo 2006 tcgtcgtttttgtcgttttgtcgt. For stimulating murine macrophages and DCs, we used as stimulatory CpG ODN1585 ggGGTCAACGTTGAGggggg, and as control, GpC ggGGTCAAGCTTGAGggggg. We also used ODN1668 tccatgacgttcct-gatgct. For mouse B cell stimulation, we used mouse-selective CpG gccat-gacgttgagct. Capital letters for ODN sequences indicate regular phosphodiester-linked nucleotides, and lowercase letters indicate phosphoro-thioate-linked nucleotides.

Cell transfection
Human Hck and Lyn siRNA SMARTpools were obtained from Dharmacon. THP-1 cells were transfected with 100 nM of each siRNA or in combination using a Nucleofector and Kit V according to the manufacturer's recommendations (Amaxa Biosystems). Cells were cultured for 48 h and then analyzed in adhesion and cytokine assays.

Cell lysis and immunoblotting
Cells were lysed in RIPA buffer for 30 min on ice (50 mM Tris, pH 7.5, 150 mM NaCl, 1% Triton X-100, 0.5% DOC, 0.1% SDS, protease inhibitor tablet [Roche], 1 mM NaF, 1 mM Na$_3$VO$_4$, and 1 mM PMSF). After centrifugation (20,000 g, 10 min, 4°C), supernatants were analyzed by SDS-PAGE. For anti-paxillin, anti-talin, and anti-vinculin immunoprecipitations, cells were lysed directly in sample buffer containing 1% SDS, boiled, and diluted 10-fold with 1% Triton X-100 containing lysis buffer.

Immunofluorescence
Cells were stimulated as indicated in figure legends and then fixed with 4% paraformaldehyde in PBS, washed twice with PBS, and blocked with 2% BSA in PBS for 2 h. All incubations and washes were performed in 0.5% BSA and 0.1% Triton X-100 in PBS. Antibody staining was performed at 37°C in a moist chamber for 1 h. F-actin was stained with FITC-phalloidin for 20 min, cells were washed twice in PBS, and nuclei were stained with TOPRO-3 for 20 min. Samples were mounted, and images were captured with a confocal microscope (IX70; Olympus) using the uPlanApo 100×/1.35 lens and Fluoview 2.0 (Olympus) program. For immobilized ODN microsphere cell binding, 10^6 microsphere beads were coated with a 1-mg/ml solution of GpC or CpG-ODN overnight and then washed four times in culture medium. Coated microspheres (10-μm diameter for RAW cells or 15 μm for peritoneal macrophages) were added to cells in culture at a microsphere/cell ratio of 3:1. Cells were fixed after an incubation of 20 min.

Adhesion assays
10^5 cells/well were plated in 96-well plates. After the indicated treatments, cells were fixed with 4% paraformaldehyde in PBS for 5 min. Unattached cells were removed by washing six times with PBS. The nuclei of attached cells were stained with Hoechst dye for 10 min. Cells were then visualized using a 5× magnification on a ArrayScanII (Cellomics), and the number of nuclei per field were counted using the manufacturer's software. For final analysis, a mean of 36 fields from at least four different wells were counted.

ELISA
Single-cell splenocyte suspensions or human pDCs (5 × 10^5 cells/well) were stimulated for 24 h with 1 μM ODN. Supernatants were collected, and IL-6 or IFN-α (R&D system) were measured by ELISA according to the manufacturer's instructions.

Flow cytometry
Splenocytes were stained and analyzed on a FACScalibur (Becton Dickinson). For measuring up-regulation of B cell activation markers, cell surface expression of CD40 and CD69 were analyzed on gated B-220–positive cells. The cells were stained with FITC-conjugated anti-CD40, anti-CD69, and allophycocyanin-conjugated anti-B220 from BD Biosciences.

Online supplemental material
Fig. S1 shows the effect of the microfilament-disrupting drugs cytochalasin D, latrunculin A, and jasplakinolide on CpG-induced adhesion. Fig. S2 shows that chloroquine and quinacrine are unable to block CpG-induced cell motility. Fig. S3 shows that MyD88$^{-/-}$ mice are unresponsive to CpG as measured by the secretion of IL-6 or the up-regulation of the plasma membrane level of CD40 and CD69. Online supplemental material is available at http://www.jcb.org/cgi/content/full/jcb.200508058/DC1.

References

Ahmad-Nejad, P., H. Hacker, M. Rutz, S. Bauer, R.M. Vabulas, and H. Wagner. 2002. Bacterial CpG-DNA and lipopolysaccharides activate Toll-like receptors at distinct cellular compartments. *Eur. J. Immunol.* 32:1958–1968.

Araiza-Casillas, R., F. Cardenas, Y. Morales, and M.H. Cardiel. 2004. Factors associated with chloroquine-induced retinopathy in rheumatic diseases. *Lupus.* 13:119–124.

Arbibe, L., J.P. Mira, N. Teusch, L. Kline, M. Guha, N. Mackman, P.J. Godowski, R.J. Ulevitch, and U.G. Knaus. 2000. Toll-like receptor 2-mediated NF-kappa B activation requires a Rac1-dependent pathway. *Nat. Immunol.* 1:533–540.

Baek, K.H., S.J. Ha, and Y.C. Sung. 2001. A novel function of phosphorothio-ate oligodeoxynucleotides as chemoattractants for primary macrophages. *J. Immunol.* 167:2847–2854.

Beaty, C.D., T.L. Franklin, Y. Uehara, and C.B. Wilson. 1994. Lipopolysaccharide-induced cytokine production in human monocytes: role of tyrosine phosphorylation in transmembrane signal transduction. *Eur. J. Immunol.* 24:1278–1284.

Bolen, J.B., and J.S. Brugge. 1997. Leukocyte protein tyrosine kinases: potential targets for drug discovery. *Annu. Rev. Immunol.* 15:371–404.

Cao, Z., W.J. Henzel, and X. Gao. 1996. IRAK: a kinase associated with the interleukin-1 receptor. *Science.* 271:1128–1131.

Carreno, S., E. Caron, C. Cougoule, L.J. Emorine, and I. Maridonneau-Parini. 2002. p59Hck isoform induces F-actin reorganization to form protrusions of the plasma membrane in a Cdc42- and Rac-dependent manner. *J. Biol. Chem.* 277:21007–21016.

Caveggion, E., S. Continolo, F.J. Pixley, E.R. Stanley, D.D. Bowtell, C.A. Lowell, and G. Berton. 2003. Expression and tyrosine phosphorylation of Cbl regulates macrophage chemokinetic and chemotactic movement. *J. Cell. Physiol.* 195:276–289.

Chiaradonna, F., L. Fontana, C. Iavarone, M.V. Carriero, G. Scholz, M.V. Barone, and M.P. Stoppelli. 1999. Urokinase receptor-dependent and -independent p56/59(hck) activation state is a molecular switch between myelomonocytic cell motility and adherence. *EMBO J.* 18:3013–3023.

Chodniewicz, D., and D.V. Zhelev. 2003. Novel pathways of F-actin polymerization in the human neutrophil. *Blood.* 102:2251–2258.

Delale, T., A. Paquin, C. Asselin-Paturel, M. Dalod, G. Brizard, E.E. Bates, P. Kastner, S. Chan, S. Akira, A. Vicari, et al. 2005. MyD88-dependent and -independent murine cytomegalovirus sensing for IFN-alpha release and initiation of immune responses in vivo. *J. Immunol.* 175:6723–6732.

Dragoi, A.M., X. Fu, S. Ivanov, P. Zhang, L. Sheng, D. Wu, G.C. Li, and W.M. Chu. 2005. DNA-PKcs, but not TLR9, is required for activation of Akt by CpG-DNA. *EMBO J.* 24:779–789.

English, B.K., J.N. Ihle, A. Myracle, and T. Yi. 1993. Hck tyrosine kinase activity modulates tumor necrosis factor production by murine macrophages. *J. Exp. Med.* 178:1017–1022.

Fox, P.L., G.M. Chisolm, and P.E. DiCorleto. 1987. Lipoprotein-mediated inhibition of endothelial cell production of platelet-derived growth factor-like protein depends on free radical lipid peroxidation. *J. Biol. Chem.* 262:6046–6054.

Franke, T.F., D.R. Kaplan, and L.C. Cantley. 1997. PI3K: downstream AKTion blocks apoptosis. *Cell.* 88:435–437.

Guo, L.H., and H.J. Schluesener. 2004. Binding and uptake of immunostimulatory CpG oligodeoxynucleotides by human neuroblastoma cells. *Oligonucleotides.* 14:287–298.

Gursel, M., D. Verthelyi, I. Gursel, K.J. Ishii, and D.M. Klinman. 2002. Differential and competitive activation of human immune cells by distinct classes of CpG oligodeoxynucleotide. *J. Leukoc. Biol.* 71:813–820.

Hacker, H., H. Mischak, T. Miethke, S. Liptay, R. Schmid, T. Sparwasser, K. Heeg, G.B. Lipford, and H. Wagner. 1998. CpG-DNA-specific activation of antigen-presenting cells requires stress kinase activity and is preceded by non-specific endocytosis and endosomal maturation. *EMBO J.* 17:6230–6240.

Jiang, Z., M. Zamanian-Daryoush, H. Nie, A.M. Silva, B.R. Williams, and X. Li. 2003. Poly(I-C)-induced Toll-like receptor 3 (TLR3)-mediated activation of NFkappa B and MAP kinase is through an interleukin-1 receptor-associated kinase (IRAK)-independent pathway employing the signaling components TLR3-TRAF6-TAK1-TAB2-PKR. *J. Biol. Chem.* 278:16713–16719.

Krieg, A.M. 2002a. A role for Toll in autoimmunity. *Nat. Immunol.* 3:423–424.

Krieg, A.M. 2002b. CpG motifs in bacterial DNA and their immune effects. *Annu. Rev. Immunol.* 20:709–760.

Krieg, A.M., A.K. Yi, S. Matson, T.J. Waldschmidt, G.A. Bishop, R. Teasdale, G.A. Koretzky, and D.M. Klinman. 1995. CpG motifs in bacterial DNA trigger direct B-cell activation. *Nature.* 374:546–549.

Latour, S., and A. Veillette. 2001. Proximal protein tyrosine kinases in immunoreceptor signaling. *Curr. Opin. Immunol.* 13:299–306.

Latz, E., A. Schoenemeyer, A. Visintin, K.A. Fitzgerald, B.G. Monks, C.F. Knetter, E. Lien, N.J. Nilsen, T. Espevik, and D.T. Golenbock. 2004. TLR9 signals after translocating from the ER to CpG DNA in the lysosome. *Nat. Immunol.* 5:190–198.

Le Cabec, V., S. Carreno, A. Moisand, C. Bordier, and I. Maridonneau-Parini. 2002. Complement receptor 3 (CD11b/CD18) mediates type I and type II phagocytosis during nonopsonic and opsonic phagocytosis, respectively. *J. Immunol.* 169:2003–2009.

Leifer, C.A., M.N. Kennedy, A. Mazzoni, C. Lee, M.J. Kruhlak, and D.M. Segal. 2004. TLR9 is localized in the endoplasmic reticulum prior to stimulation. *J. Immunol.* 173:1179–1183.

Li, S., A. Strelow, E.J. Fontana, and H. Wesche. 2002. IRAK-4: a novel member of the IRAK family with the properties of an IRAK-kinase. *Proc. Natl. Acad. Sci. USA.* 99:5567–5572.

Lutz, M.B., N. Kukutsch, A.L. Ogilvie, S. Rossner, F. Koch, N. Romani, and G. Schuler. 1999. An advanced culture method for generating large quantities of highly pure dendritic cells from mouse bone marrow. *J. Immunol. Methods.* 223:77–92.

Macfarlane, D.E., and L. Manzel. 1998. Antagonism of immunostimulatory CpG-oligodeoxynucleotides by quinacrine, chloroquine, and structurally related compounds. *J. Immunol.* 160:1122–1131.

Manzel, L., and D.E. Macfarlane. 1999. Lack of immune stimulation by immobilized CpG-oligodeoxynucleotide. *Antisense Nucleic Acid Drug Dev.* 9:459–464.

Mercurio, F., H. Zhu, B.W. Murray, A. Shevchenko, B.L. Bennett, J. Li, D.B. Young, M. Barbosa, M. Mann, A. Manning, and A. Rao. 1997. IKK-1 and IKK-2: cytokine-activated IkappaB kinases essential for NF-kappaB activation. *Science.* 278:860–866.

Mitra, S.K., D.A. Hanson, and D.D. Schlaepfer. 2005. Focal adhesion kinase: in command and control of cell motility. *Nat. Rev. Mol. Cell Biol.* 6:56–68.

Nayal, A., D.J. Webb, and A.F. Horwitz. 2004. Talin: an emerging focal point of adhesion dynamics. *Curr. Opin. Cell Biol.* 16:94–98.

Nederman, T., E. Karlstrom, and L. Sjodin. 1990. An in vitro bioassay for quantitation of human interferons by measurements of antiproliferative activity on a continuous human lymphoma cell line. *Biologicals.* 18:29–34.

Neumann, D., S. Lienenklaus, O. Rosati, and M.U. Martin. 2002. IL-1beta-induced phosphorylation of PKB/Akt depends on the presence of IRAK-1. *Eur. J. Immunol.* 32:3689–3698.

Nord, J.E., P.K. Shah, R.Z. Rinaldi, and M.H. Weisman. 2004. Hydroxychloroquine cardiotoxicity in systemic lupus erythematosus: a report of 2 cases and review of the literature. *Semin. Arthritis Rheum.* 33:336–351.

Regnier, C.H., H.Y. Song, X. Gao, D.V. Goeddel, Z. Cao, and M. Rothe. 1997. Identification and characterization of an IkappaB kinase. *Cell.* 90:373–383.

Resnati, M., M. Guttinger, S. Valcamonica, N. Sidenius, F. Blasi, and F. Fazioli. 1996. Proteolytic cleavage of the urokinase receptor substitutes for the agonist-induced chemotactic effect. *EMBO J.* 15:1572–1582.

Rogers, N.C., E.C. Slack, A.D. Edwards, M.A. Nolte, O. Schulz, E. Schweighoffer, D.L. Williams, S. Gordon, V.L. Tybulewicz, G.D. Brown, and C. Reis e Sousa. 2005. Syk-dependent cytokine induction by Dectin-1 reveals a novel pattern recognition pathway for C type lectins. *Immunity.* 22:507–517.

Rutz, M., J. Metzger, T. Gellert, P. Luppa, G.B. Lipford, H. Wagner, and S. Bauer. 2004. Toll-like receptor 9 binds single-stranded CpG-DNA in a sequence- and pH-dependent manner. *Eur. J. Immunol.* 34:2541–2550.

Sarkar, S.N., K.L. Peters, C.P. Elco, S. Sakamoto, S. Pal, and G.C. Sen. 2004. Novel roles of TLR3 tyrosine phosphorylation and PI3 kinase in double-stranded RNA signaling. *Nat. Struct. Mol. Biol.* 11:1060–1067.

Scholz, G., K. Cartledge, and A.R. Dunn. 2000. Hck enhances the adherence of lipopolysaccharide-stimulated macrophages via Cbl and phosphatidyl-inositol 3-kinase. *J. Biol. Chem.* 275:14615–14623.

Stovall, S.H., A.K. Yi, E.A. Meals, A.J. Talati, S.A. Godambe, and B.K. English. 2004. Role of vav1- and src-related tyrosine kinases in macrophage activation by CpG DNA. *J. Biol. Chem.* 279:13809–13816.

Strekowski, L., O. Zegrocka, M. Henary, M. Say, M.J. Mokrosz, B.M. Kotecka, L. Manzel, and D.E. Macfarlane. 1999. Structure–activity relationship analysis of substituted 4-quinolinamines, antagonists of immunostimulatory CpG-oligodeoxynucleotides. *Bioorg. Med. Chem. Lett.* 9:1819–1824.

Suen, P.W., D. Ilic, E. Caveggion, G. Berton, C.H. Damsky, and C.A. Lowell. 1999. Impaired integrin-mediated signal transduction, altered cytoskeletal structure and reduced motility in Hck/Fgr deficient macrophages. *J. Cell Sci.* 112:4067–4078.

Suzuki, T., H. Kono, N. Hirose, M. Okada, T. Yamamoto, K. Yamamoto, and Z. Honda. 2000. Differential involvement of Src family kinases in Fcγ receptor-mediated phagocytosis. *J. Immunol.* 165:473–482.

Takeda, K., and S. Akira. 2005. Toll-like receptors in innate immunity. *Int. Immunol.* 17:1–14.

Takeda, K., T. Kaisho, and S. Akira. 2003. Toll-like receptors. *Annu. Rev. Immunol.* 21:335–376.

Trape, J.F., G. Pison, A. Spiegel, C. Enel, and C. Rogier. 2002. Combating malaria in Africa. *Trends Parasitol.* 18:224–230.

Trinchieri, G. 2003. Interleukin-12 and the regulation of innate resistance and adaptive immunity. *Nat. Rev. Immunol.* 3:133–146.

Tybulewicz, V.L., L. Ardouin, A. Prisco, and L.F. Reynolds. 2003. Vav1: a key signal transducer downstream of the TCR. *Immunol. Rev.* 192:42–52.

Verthelyi, D., and R.A. Zeuner. 2003. Differential signaling by CpG DNA in DCs and B cells: not just TLR9. *Trends Immunol.* 24:519–522.

Vincent, M.S., D.S. Leslie, J.E. Gumperz, X. Xiong, E.P. Grant, and M.B. Brenner. 2002. CD1-dependent dendritic cell instruction. *Nat. Immunol.* 3:1163–1168.

Vollmer, J., R. Weeratna, P. Payette, M. Jurk, C. Schetter, M. Laucht, T. Wader, S. Tluk, M. Liu, H.L. Davis, and A.M. Krieg. 2004. Characterization of three CpG oligodeoxynucleotide classes with distinct immunostimulatory activities. *Eur. J. Immunol.* 34:251–262.

Wallace, D.J. 2001. Antimalarials—the 'real' advance in lupus. *Lupus.* 10:385–387.

Weinstein, S.L., M.R. Gold, and A.L. DeFranco. 1991. Bacterial lipopolysaccharide stimulates protein tyrosine phosphorylation in macrophages. *Proc. Natl. Acad. Sci. USA.* 88:4148–4152.

Wesche, H., W.J. Henzel, W. Shillinglaw, S. Li, and Z. Cao. 1997. MyD88: an adapter that recruits IRAK to the IL-1 receptor complex. *Immunity.* 7:837–847.